Chaos, Solitons and Fractals 158 (2022) 112099

Contents lists available at ScienceDirect

Chaos, Solitons and Fractals

Nonlinear Science, and Nonequilibrium and Complex Phenomena

journal homepage: www.elsevier.com/locate/chaos

Stabilization of an unstable equilibrium of a balance platform due to short-term training

Nikita S. Frolov [a,b], Vladimir S. Khorev [b], Vadim V. Grubov [a,b], Artem A. Badarin [a,b], Semen A. Kurkin [a,b], Vladimir A. Maksimenko [a,b], Alexander E. Hramov [a,b], Alexander N. Pisarchik [b,c,*]

[a] Center for Neurotechnology and Machine Learning, Immanuel Kant Baltic Federal University, 236041 Kaliningrad, Russia
[b] Neuroscience and Cognitive Technology Laboratory, Center for Technologies in Robotics and Mechatronics Components, Innopolis University, 420500 Innopolis, Russia
[c] Centre for Biomedical Technology, Universidad Politécnica de Madrid, 28223 Madrid, Spain

ARTICLE INFO

Article history:
Received 9 March 2022
Accepted 6 April 2022
Available online xxxx

Keywords:
Control
Balance
Mathematical model
EMG
Training
Data analysis

ABSTRACT

We study experimentally and numerically the dynamics of a balance platform during a short-term training. The results of experiments with sixteen untrained subjects and a developed empirical biomechanical model exhibit the coexistence of three attractors under adaptive control of multistability. During the experiments, we measure the balance bar angle, angular velocity, and angular acceleration. Simultaneously, superficial electromyography (EMG) is recorded on the flexors and extensors of the ankle and knee joints. Phase-space analysis of the platform movement shows that the time the platform spends near the unstable equilibrium correlates with the average muscle activity. We also observe that the balance platform dynamics differs when the subject starts balancing with his/her dominant or non-dominant leg. In addition, we find that subjects with better symmetry between the strength of dominant and non-dominant legs demonstrate higher training efficiency. Therefore, the balance control efficiency can be enhanced by training muscles of the non-dominant leg. The results of numerical simulations are in good agreement with experiments.

1. Introduction

Multistability or the coexistence of several asymptotic states (attractors) for a given set of parameters is one of the most exciting phenomena in physical and living systems [1–5]. A set of initial conditions that asymptotically approach an attractor is called basin of attraction. When there are two different attractors in a certain region of phase space, there are two basins separated by a basin boundary which can be either smooth or fractal. The study of these basins can provide much information about the system since their topology is deeply related to the dynamical nature of the system. However, for open systems, where the concept of attractors or basins of attraction is meaningless, we can still define escape basins in an analogous way to the basins of attraction in a dissipative system. An escape (or exit) basin is the set of initial conditions that escapes through a certain exit [6].

Multistability can be useful for some applications, e.g., logic gates [7] and secure communications [8], where switching between coexisting states improves the system performance. On the other hand, multistability can be undesirable in a robust-to-noise device with predominant output characteristics. Therefore, the development of efficient strategies for controlling multistability is an actual problem in science and engineering [9,10]. The control aims can include (i) creation of new attractors, (ii) annihilation of undesirable attractors, (iii) changing the attractor properties (type, stability), and (iv) modification of basins of attraction.

In this work, we focus on a practical problem of using muscular activity of the human body to control multistability of a balance platform, in particular, to stabilize an unstable equilibrium. Many physiological processes in the human body participate in controlling balance [11]. Numerous clinical studies show that the balance function is very complex [12–15]. Many researchers examine various features of the postural response with different support surfaces located under the foot [16–18]. In this regard, short-term training plays important role. The balance component of training performed on unstable surfaces appears to activate stabilizing core muscles and trigger stabilizing motor functions [19,20].

It should be noted that differences in function or performance between dominant and non-dominant limbs during balance exercises are common [21]. The bilateral asymmetry in the lower-limb strength is known [22] to affect dynamical balance [21,23]. While the dominant leg can handle a lot of muscle and tendon stress during sports, another

* Corresponding author at: Centre for Biomedical Technology, Universidad Politécnica de Madrid, 28223 Madrid, Spain.
E-mail address: alexander.pisarchik@ctb.upm.es (A.N. Pisarchik).

https://doi.org/10.1016/j.chaos.2022.112099

leg may not be able to handle even a moderate load [24]. This often causes an increased risk of sport injuries [25,26]. The key difference between the present research and the majority of other experimental studies is that here we investigate the imbalance in the muscle activity caused by the subject himself in the short term, and not during long multi-week training. The concept of a voluntary goal allows an individual to actively seek an effective control strategy. Another positive aspect of the voluntary goal approach is its similarity to real-time exercises, as people usually willingly participate in tasks that require physical activity. Throughout the training, the error in choosing the correct strategy gradually decreases, demonstrating first a fairly rapid improvement [27], and then the training efficiency slows down and saturates.

For proper planning of the training process, it is very important to know how the person's physical activity adapts during short-term training. Therefore, the main aim of this work is to study how the short-term balance training affects the efficiency in controlling multistability of a balance platform. To do this, we analyze the platform dynamics during the balance experiment and investigate the relationship between muscle activity and behavioral characteristics.

2. Methods

2.1. Participants

Sixteen healthy male volunteers (29.6 ± 6.0 years old, weight 71.0 ± 13.3 kg) were recruited from the staff and undergraduate students of the Innopolis University to participate in this study. According to the Waterloo Footedness Questionnaire-Revised [28,29], all subjects had the right dominant. The participants had no history of neurological pathologies, i.e., stroke, tumors, head injuries. All volunteers were new to the experimental paradigm and signed written informed consent beforehand. The experimental study was approved by the local Ethics Committee and performed in accordance with the Declaration of Helsinki.

2.2. Body balance training

To study the training effect, we conducted a series of experiments in which subjects were placed on a specially designed 1-m length balancing board, as illustrated in Fig. 1A. A detailed description of the board can be found in Supplementary Materials. The difficulty of balancing can be controlled with a spring compressing the hinge. The sliding friction force of the spring was equal to 25 N (the most difficult option). The rotation angle of the balance board, velocity, and acceleration were simultaneously recorded by the accelerometer sensor LIS331DLH [30]. A pilot study was carried out in the morning and afternoon periods (9:00 am to 1:00 pm) 2 h after a healthy meal with limited caffeine and (or) other stimulant supplements. The experimental design included three 10-min sessions with two rest breaks in between (see Fig. 1C). The preliminary registration of the background (BG) subject activity without performing special instructions was carried out for 5 min in a standing position on the floor. All subjects were instructed to keep an upright body position while trying to maintain balance on the platform Fig. 2A, B. A typical subject posture during the experiment on the board is shown in Fig. 1A. Since the body is in unstable equilibrium due to a small fulcrum and a high location of the body mass center, even minor impacts can upset the balance and cause the platform to touch the frame balancer.

2.3. Electrophysiological assessment

To assess muscle activity, we recorded surface EMG signals during the experimental session. As shown in the EMG layout in Fig. 1B, the activity of the following muscles was recorded: tibialis anterior (TA), gastrocnemius medial head (GM), rectus femoris straight head (RF), and semitendinosus (ST). The prefixes L and R in muscle contraction denote left and right sides, respectively (e.g., LTA – Left Tibialis Anterior).

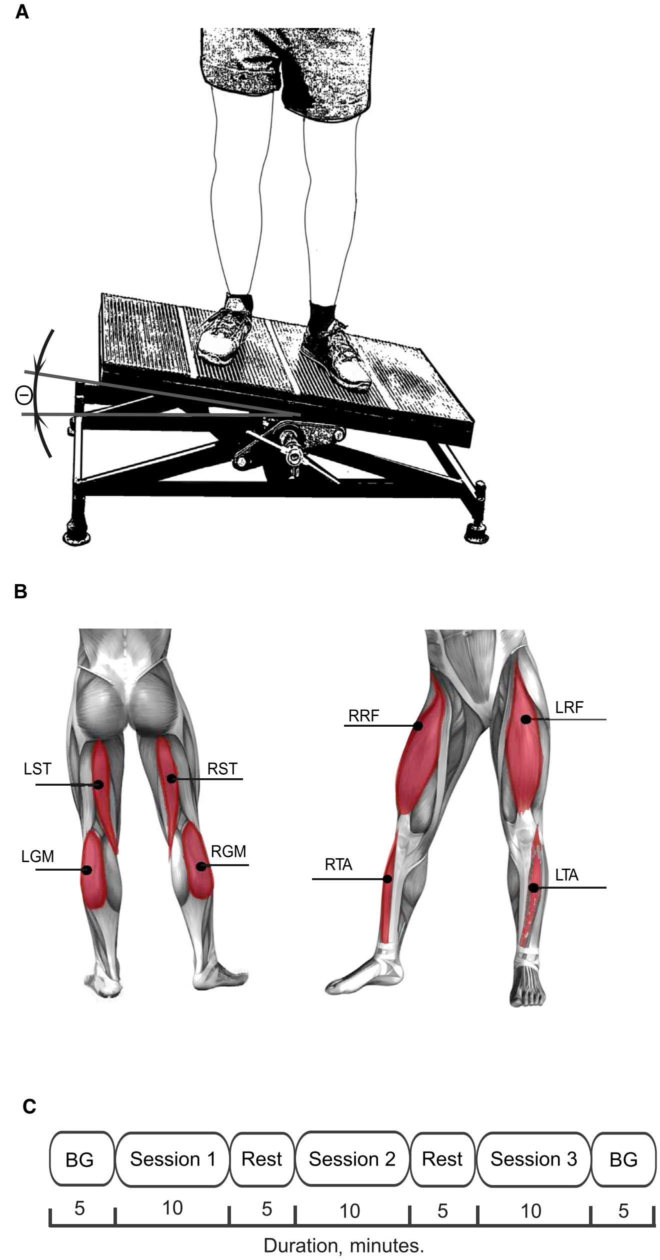

Fig. 1. Experimental schemes. A. Balance board (θ is the platform angle). B. EMG electrode placement. Left/Right Rectus Femoris (LRF/RRF), Left/Right Tibialis Anterior (LTA/RTA), Left/Right Semitendinosus (LST/RST), Left/Right Gastrocnemius (LGM/RGM). C. Experimental timeline. BG denotes background activity.

One flexor and one extensor for each part of the leg, which provide maximum control of the shin and ankle [31]. Before placing the electrodes, the subject was instructed on how to selectively activate each muscle [32] in order to optimize the EMG signal and minimize crosstalk from adjacent muscles during isometric contractions. Fig. 1C shows the signals acquired using pre-gel disposable electrodes Swaromed 1036 (Vermed, Austria) with a silver/silver chloride sensor placed on the skin aver the muscles. The impedance was controlled in the range of 2–5 kΩ throughout the experiments, data sampling rate for the signals was 250 Hz. In the experiment, we used an Encephalan-EEG-19/26 device (Medicom MTD, Taganrog, Russian Federation) with a set of A-5364 cables for EMG derivations. This device held FCP 2007/00124 from 07/11/2014 and European CE 538571 from British Standards Institute. Data containing EMG signals and balance board angle are available at [33] location.

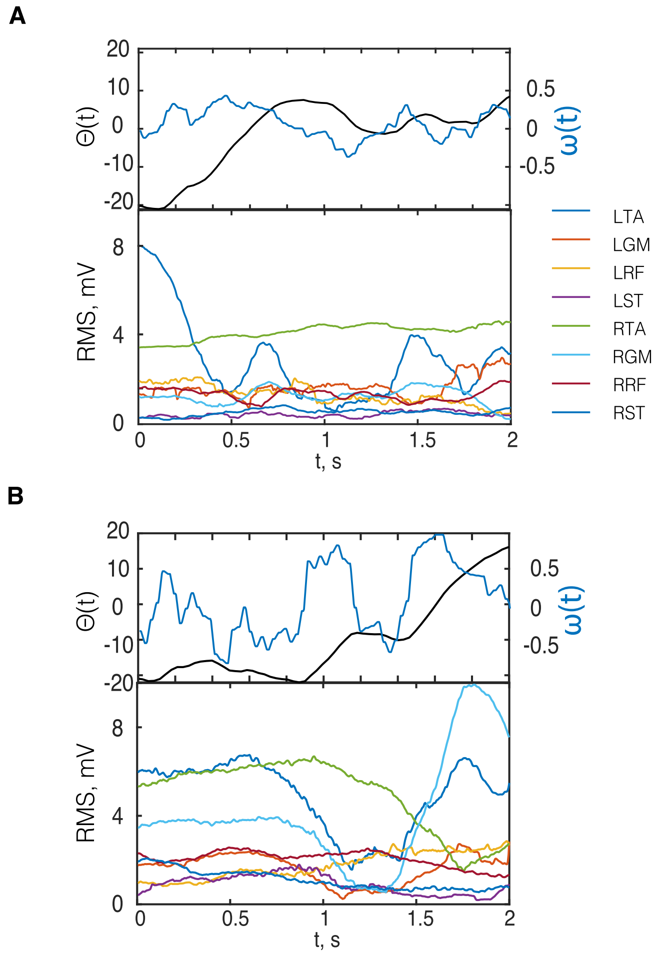

Fig. 2. Time series. A. Root-mean square (RMS) of the surface EMG recordings during a successful balance keeping attempt, balance platform angle and angular velocity (ω). B. Root-mean square of the surface EMG recordings during an unsuccessful balance keeping attempt, balance platform angle and angular velocity.

2.4. Data analyses

2.4.1. Board kinematics and phase space analysis

Considering the 10-min time series of changes in the balance board angle variation $\theta(t_i)$ in sessions $s = 1,2,3$, we first numerically estimated the angular velocity $\omega(t_i)$ as the first derivative of the angle $\omega_s(t_i) = \dot{\underset{s}{\theta}}(t_i), s = 1, 2, 3 (i = 2, \ldots, T)$. Due to the intersubjective variability of the angular velocity, for all participants in a similar way to the z-score. In each session, we standardize the angular velocity by dividing each value $\omega_s(t_i)$ of the time series by the standard deviation of the angular velocity in the first session $\sigma(\omega_1)$:

$$\omega'_s(t_i) = \omega_s(t_i)/\sigma(\omega_1) \tag{1}$$

The angular acceleration $\psi_s(t_i)$ was then calculated as the first derivative of the standardized angular velocity.

Orbital trajectories of the balance platform motion were analyzed in the two-dimensional phase space (θ_s, ω') formed by the variables of the platform angle and its standardized angular velocity. Further nonlinear analyze based on this phase-space representation included quantification of the attractors' potential and capture time, i.e., the total amount of time, during which the trajectory is trapped in the basin of attraction of the potential well.

The motion of the platform without the presence of a human corresponds to the dissipative system, which can be described by the model of particle motion with two potential wells. The configuration of the basins of attraction is schematically represented in Fig. 4 along with the phase trajectories for successful and unsuccessful attempts. Although an unstable position is theoretically possible without controller, practically the platform will tend either to the left or to the extreme right position. The presence of a human actively controlling the platform's speed and angle leads to the appearance of a potential well near the unstable equilibrium, *NSE*, which corresponds to the one schematically depicted in Fig. 3B. The width and depth of the potential well near the unstable equilibrium state is an estimate of the level of control of the system state. The full orbital trajectory of the balance platform motion in sessions 1, 2, and 3 are shown in Fig. 5A).

Assuming the control function over platform angle executed by the human $F(\theta_s(t))$, we can expect to see the changes in the angle distributions. At the initial moment t_0 the system is in the state $(\theta(t_0), \omega_s{}'(t_0))$ (angle and velocity), it is necessary to determine such a control $F(t)$, which will move the system to a given final state $(\theta_{eq}(T), \omega_{eq}{}'(T))$ different from the initial state, ideally both should equal to zero in balanced system), where $T < \infty$ is a finite time. It is usually required that the transition from a point $(\theta(t_0), \omega_s{}'(t_0))$ to a point $(\theta(T), \omega'(T))$ (the transition process) is in some sense the best of all possible transitions. For example, if technical system is considered, then the transition process must satisfy the condition of minimum spent energy or the condition of minimum transition time. This best transient process is called an optimal process. A control function $F(t)$ usually belongs to some control area, which is a set within Euclidean space. In technical applications, it is assumed that the region of control area is a closed region, the region including its boundaries. An admissible control is any control $F(t)$, which transfers the system from a point $(\theta(t_0), \omega_s{}'(t_0))$ to a point $(\theta(T), \omega'(T))$. For quantitative comparison of various admissible controls, we introduce an optimality criterion, which can be presented in the form of the following function

$$I = \int_0^T H(\theta(t), \omega'_s(t), F(t))dt \tag{2}$$

The adaptive control can be considered optimal among all admissible controls, which move the phase-space point from $(\theta(t_0), \omega_s{}'(t_0))$ to the point $(\theta(T), \omega'(T))$, for which the function Eq. (2) has the lowest value [34]. For the fixed discretization step, we can present the movement function as a map where $\theta_{n+1} = \theta(t_{n+1}), \omega_{n+1}{}' = \omega'(t_{n+1})$, so

$$(\theta_{n+1}, \omega'_{n+1}) = f(\theta_n, \omega'_n) + \delta \tag{3}$$

where δ denotes a random process. We can define a spherical neighborhood of radius ρ around the attractor. As soon as the trajectory falls into this neighborhood, the control is switched on to keep the system close to this attractor despite the noise. Assuming that the ρ-neighborhood is small enough so that the linearization is valid, we can control the trajectory by adding a control term in the form of

$$\left(\widehat{\theta}_{n+1}, \widehat{\omega}'_{n+1}\right) = (\theta_{n+1} + C_1\varepsilon, \omega'_{n+1} + C_2\varepsilon) \tag{4}$$

where $C_{1,\,2}$ is the control vector and ε denotes the distance from the fixed point.

The problem of a real system is the absence of analytical solutions for the control function $F(t)$. However, it is reasonable to assume partial human control over the velocity and angle of the system. If the velocity at the initial segment of the phase trajectory is insufficient, the system returns to its initial position, which is comparable to the particle motion in the segment until the unstable equilibrium is reached. If the velocity is too high, the system makes a transition from one stable equilibrium to another, which corresponds to the particle passing through the region corresponding to the unstable equilibrium position, and overstepping its limits. Controlling the velocity to keep the particle in the region of unstable equilibrium allows it to be in the central region. The proposed

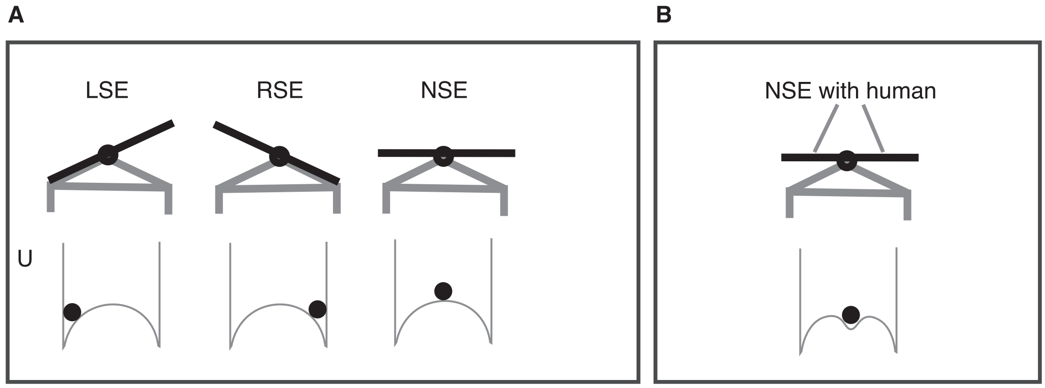

Fig. 3. Equilibrium configuration. A. Left/Right stable equilibrium positions (LSE/RSE) and unstable equilibrium position (NSE) of the balance board. Illustrative potential landscapes for each equilibrium position are shown below. B. Potential landscape for the unstable equilibrium position with human control.

phase-space configuration of the system initial state without human intervention includes two fixed points corresponding to stable equilibria, as well as a saddle point corresponding to an unstable equilibria. In the presence of a human controller, the stability of a saddle point is changed because it is transformed into a stable equilibrium, and two additional saddle points appear between the new stable fixed point and two remaining stable equilibria. Thus, due to adaptive control the bistable dynamical system is converted into a tristable system.

In deterministic autonomous dynamical systems, the phase-space trajectory never crosses basin boundaries. Depending on initial conditions, the trajectory always remains in a particular basin of attraction and asymptotically converges to the attractor. A different situation occurs in nonautonomous systems. An external forcing can push the trajectory out of the basin, so that the position and stability of steady states change. When the trajectory moves along the phase space, the moving separatrix can overtake it. This event is called a capture. When a capture occurs, the affected trajectory is deviated, and often exhibits a sudden change in direction, since it is now attracted to a different attractor at a different position of phase space than it was before. Captures will happen when the flow along the trajectory is less than the rate of change in the separatrix position. The separatrix is recruiting points from one basin of attraction to another faster than the trajectory moves away from it [35].

2.4.2. Potential landscape analysis

We analyze the potential function to quantify the effect of training on stabilizing the unstable equilibrium, *NSE* (see Fig. 1F). This approach is commonly used in ecological [36,37] and biological systems [38,39].

Let us assume that the platform rotation under human control, i.e. the variation of the angle $\theta_s(t)$ throughout a single session, is a homogeneous process. It can be represented as a generic one-dimensional random process $X(t)$ driven by a stochastic term, a Wiener process $W(t)$. The evolution of $X(t)$ is therefore governed by a stochastic differential equation

$$dX(t) = -U'(X,t)dt + DdW(t) \tag{5}$$

where $U(t)$ is a potential function providing the drift of $X(t)$, $D=\sigma^2/2$ is a diffusion coefficient, and σ is a standard deviation of $X(t)$. Eq. (5) can be solved by introducing an appropriate probability function $p(x,t)$ and writing a corresponding Fokker-Planck equation:

$$\frac{\partial}{\partial t}p(x,t) = \frac{\partial}{\partial x}\left[U'(x,t)p(x,t)\right] + \frac{\partial^2}{\partial x^2}\left[D(x,t)p(x,t)\right] \tag{6}$$

Since we are interested in the stationary solution of Eq. (6), we assume $\partial p(x,t)/\partial t = 0$ to obtain the ordinary differential equation

$$\frac{\partial}{\partial x}\left[U'(x)p(x)\right] + D\frac{\partial^2}{\partial x^2}p(x) = 0$$

equivalent to

$$\frac{U'(x)}{D}p(x) + \frac{\partial}{\partial x}p(x) = 0 \tag{7}$$

The stationary solution is found from Eq. (7) as $p(x) = \exp\left[-U(x)/D\right]$, which can be rewritten in terms of potential:

$$U(x) = -D\log\left[p(x)\right] = -\frac{\sigma^2}{2}\log\left[p(x)\right] \tag{8}$$

Resulting Eq. (8) expresses the potential function of a generic random process $X(t)$ given the probability $p(X=x)$ and standard deviation $\sigma(X)$. Then, we replace $X(t)=\theta_s(t)$ and use Eq. (8) to construct the potential landscape of the balance platform motion during a single experimental session.

According to Hirota et al. [37] and Curtin et al. [39], the potential energy is presented in the normalized units $U(\theta_s)/\sigma^2(\theta_s)$. The analysis establishes the presence of three equilibria characterized by a local minima and a local maximum of potential energy: (i) right-side stable equilibrium, *RSE*, with a minimum around $+20°$; (ii) left-side stable equilibrium, *LSE*, with a minimum around $-20°$; and (iii) unstable equilibrium, *NSE*, with a maximum around 0° (all positions can be seen in Fig. 3).

2.4.3. Preprocessing of EMG data

The raw EMG signals were filtered using a band-pass filter with 1-Hz (LF) and 10-Hz (HF) cutoff frequencies.

To analyze the set of muscle fibers during contraction, we used evaluators of various EMG amplitude, among which the most common is the root-mean-square (*RMS*). This is a linear variable used to assess muscle excitability and activation [40,41]. The time-dependent *RMS* of the EMG signal $x_s(t_i)$ was calculated in a floating window as

$$RMS_{x,s}(t_i) = \sqrt{\frac{1}{w}\sum_{j=i-w/2}^{i+w/2} x_s(t_j)}, \quad s=1,2,3, i=w/2+1,\ldots,T-w/2 \tag{9}$$

where $w=25$ data points is the floating window width. Since the obtained result $RMS_{x,\ s}(t_i)$ has a positively skewed distribution and strong inter-subject variability of the means, it was normalized and standardized as follows. First, cube root normalization was applied to $RMS_{x,\ s}(t_i)$ to avoid positive skewness. Then, the normalized time series $RMS^n_{x,s}$ were standardized in each session similar to the z-score as follows

$$RMS'_{x,s}(t_i) = \frac{RMS^n_{x,s}(t_i) - \overline{RMS^n_{x,s}}}{\sigma(RMS^n_{x,1}), \quad s = 1,2,3} \tag{10}$$

$$RMS^n_{x,s}(t_i) = RMS_{x,s}(t_i)^{1/3}, \quad s = 1,2,3 \tag{11}$$

2.4.4. Epoching

In order to analyze the loss of asymmetry of trajectories from the right stable equilibrium ($RSE \approx +20^\circ$) and left stable equilibrium ($LSE \approx -20^\circ$, Fig. 3), we conducted the epoching of the orbital trajectories and the corresponding RMS' time series. In each session, we collected epochs of (a) successful attempt trajectories starting at either *RSE* or *LSE* and up to *NSE* (red arrows in Fig. 6C) and (b) unsuccessful attempt trajectories starting at either *RSE* or *LSE* and reaching their counterpart stable state through *NSE* (blue arrows in Fig. 6C). The duration of each epoch was 1.5 s. The orbital trajectories and RMS' were then averaged over the collected epochs for each participant.

2.5. Statistical analyses

Changes in mean potential energy, trapping time, and mean PDF of the standardized velocity of the *NSE* attractor during training were assessed using repeated measures analysis of variance, RM ANOVA. The sphericity assumption was taken into account using the Greenhouse–Geisser correction. Post-hoc analysis was performed using the paired sample *t*-test with Holm correction for multiple comparisons.

To quantify the interaction of intra-subject factors Session*Side on orbital trajectories, we performed the RM ANOVA analysis at each phase-space point using the time series, resulting in a time-dependent *F*-value. Thus, the time interval during which *F* exceeds the critical value corresponding to a given alpha-level should have a significant interaction effect.

The group-level correlation between the observed changes in orbital trajectories of the platform motion and the corresponding muscular activation was quantified using the repeated measures correlation, RM CORR [42] with the JASP statistical package [43].

3. Results

3.1. Phase space analysis of the balance platform motion

A series of experiments were conducted with sixteen subjects, who were asked to maintain balance on a specially designed balancing platform (see Fig. 1A). To determine dynamical features of the platform motion, we analyzed the platform position, such as its angle θ, angular velocity $\omega = d\theta/dt$, and angular acceleration $d\omega/dt$. Then, we considered the balance platform movement as a trajectory in the phase space of two variables, the angle θ and standardized angular velocity ω'.

Numerical simulations using the Fokker–Planck equation allowed us to calculate a potential energy landscape with respect to θ (see Methods, Eq. (8)). The resulting group means ± SD of the potential energy landscapes in each session are plotted in the left panel in Fig. 5A. Here, *RSE* and *LSE* are referred to as right and left attractors since they denote two stable boundary positions, in which one of the platform edges rests on the pedestal frame (equilibrium positions are shown in Fig. 3). On the contrary, *NSE* is referred to as unstable equilibrium since the equilibrium is only possible here under the participant's control via body balance maintenance. Eventually, the trajectory leaves the *NSE* state and converges to either *LSE* or *RSE*.

Based on the potential landscape construction, we determined the boundaries of the *NSE* attractor and estimated its mean potential energy in each session for each participant. Accordingly, we estimated the trapping time of the *NSE* attractor as the sum of all points in the phase space lying within its boundaries, multiplied by the time resolution $\Delta t = 0.004$ s.

$$T_{trap} = \sum_{1}^{N} \left[(|\theta_s| \le \theta_e) \wedge (|\omega'_s| \le \omega_e) \right] \Delta t \tag{12}$$

where N is the time series length, θ_e is the critical equilibrium boundary angle, set to 10° as a result of the potential reconstruction analysis (similar points of decline are shown in Fig. 5A), $\omega_e = 0.5$ is the maximal velocity in the vicinity of the unstable equilibrium *NSE*. Therefore, the capture is represented in the appropriate physical units (in seconds) (see Table 1).

From Fig. 4A we can conclude that the potential well of the *NSE* state becomes deeper with training. This means that the unstable equilibrium is stabilized for a short time due to adaptive human control. Determining the *NSE* boundaries from -10° to $+10^\circ$, we calculated the mean potential energy of the *NSE* equilibrium in sessions S1, S2, and S3. RM ANOVA demonstrates a strong influence of the session on the mean potential energy (see Table 2). The mean values of the groups and SDs are presented in the right panel in Fig. 5A.

To determine the *NSE* boundaries in terms of ω', we analyzed the probability density function of ω' near the *NSE* equilibrium in sessions S1, S2, and S3 (left panel in Fig. 1B). One can see that the group-mean PDF curves intersect at about -0.5 and $+0.5$ SD of the angular velocity, that determines the required boundaries. Considering mean PDFs within the specified boundaries, RM ANOVA shows that SD of the angular velocity is strongly affected by the session factor (see Table 2). The group means and SDs are plotted in the right panel in Fig. 5B.

Considering the full orbital trajectory of the balance platform motion in sessions 1, 2, and 3, we observe an increase in the density of points in the vicinity of the *NSE* state from S1 to S3 (Fig. 6A). This allows us to conclude that as the training progresses, the trajectory recures the *NSE* more frequently and remains there for a longer time. Indeed, RM ANOVA demonstrates that the time to capture the *NSE* region (see Methods) strongly depends on the session factor (Greenhouse–Geisser corrected). Group means and SDs are presented in Fig. 6B.

In general, we are able to interpret the observed potential well deepening, the decrease in the angular velocity near the *NSE*, and the increase in the trapping time as stabilization of the platform unstable equilibrium during ongoing training sessions. These observations most likely indicate the development of body balance skills that improve control of the platform movement near the unstable equilibrium.

Table 1
Subjects' weight, age, and trapping times for S1, S2, and S3 sessions.

Subject	Weight, kg	Age, years	T_{trap} in session S1, s	T_{trap} in session S2, s	T_{trap} in session S3, s
1	79	27	110.58	119.73	209.91
2	61	26	238.89	251.23	386.46
3	70	24	97.85	197.34	304.75
4	80	45	107.74	110.26	173.20
5	72	33	185.90	205.72	185,34
6	65	27	182,68	339,94	379.76
7	55	22	203.09	310.13	490.36
8	73	31	146.41	314.85	409.62
9	91	40	86.65	122,58	165.45
10	60	25	91.23	119.18	141.40
11	85	34	107.02	167.88	206.68
12	95	32	91.92	164.53	189.18
13	64	27	315.96	311.71	285.96
14	92	31	71.93	95.25	83.13
15	64	24	150.47	207.78	264.18
16	49	25	230.45	288.58	367.02
Mean ± SD	71.0 ± 13.3	29.6 ± 6.0	151.2 ± 56.2	207.9 ± 71.1	265.1 ± 95.9

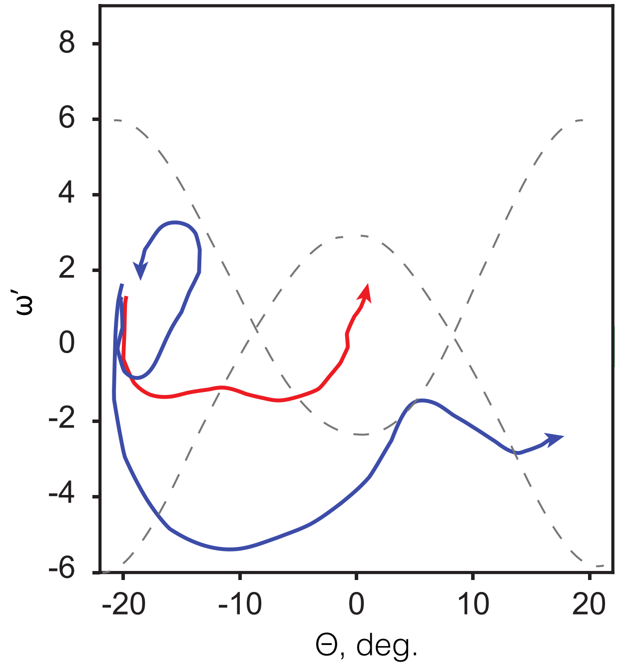

Fig. 4. Phase trajectories. Successful (red) and unsuccessful (blue) trajectories of one of the subjects reaching stable and unstable equilibria, assumed separatrix is showed by the dash line. (For interpretation of the references to colour in this figure legend, the reader is referred to the web version of this article.)

3.2. Analysis of movement trajectories asymmetry and muscle activity

To gain a deeper understanding of the dynamics and associated muscle control underlying the observed stabilization of the *NSE* equilibrium, let us to turn back to Fig. 6C. One can see that the trajectory of the platform movement has a strong asymmetry of the angular velocity in session S1, and gradually disappears in S2 and S3. This asymmetry results in higher angular velocity of the trajectory leaving the *RSE* attractor than the trajectory leaving the *LSE*. Although Fig. 6C shows approximate individual trajectories obtained from subject 1. The described phenomenon is common to the entire group of participants. Based on this observation, we hypothesize that short-term body balance training develops platform trajectory control and reduces the associated functional asymmetry of the human body [44]. Improved angular velocity control should contribute to more reliable trajectory convergence to the *NSE* equilibrium, which improves the overall performance of the body balance exercise.

Table 2
RM ANOVA and post-hoc analyses of the mean potential energy $\overline{U}$, standardized angular velocityω' near the *NSE* state, and trapping time T_{trap}.

Variable	Factor	$F_{2,\,30}$	p	η^2
$\overline{U}$	Session	31.79	<0.001	0.68
Session	Difference	t	p	d
S1-S2	0.074	5.18	<0.001	1.30
S2-S3	0.038	2.66	0.012	0.67
S1-S3	0.11	7.84	<0.001	1.96
Variable	Factor	$F_{2,\,30}$	p	η^2
ω'	Session	21.49	<0.001	0.59
Session	difference	t	p	d
S1-S2	0.063	−4.02	<0.001	1.01
S2-S3	0.039	−2.47	0.019	−0.62
S1-S3	0.101	−6.49	<0.001	−1.62
Variable	Factor	$F_{1.23,19.49}$	p	η^2
T_{trap}	Session	22.10	<0.001	0.60
Session	difference	t	p	d
S1-S2	56.75	−3.31	0.005	−0.83
S2-S3	57.23	−3.34	0.005	−0.83
S1-S3	113.98	−6.65	<0.001	−1.66

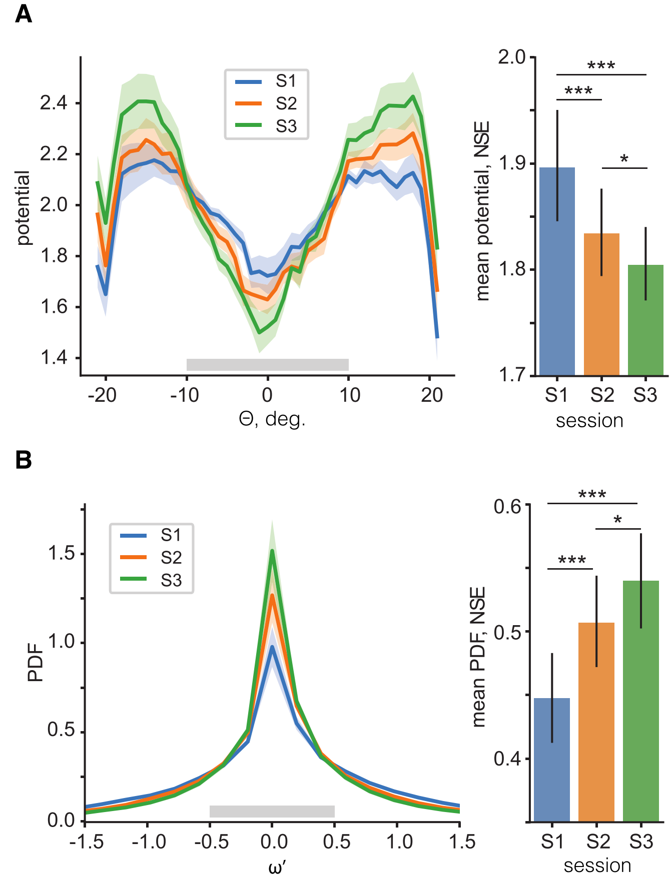

Fig. 5. Potential analysis of the platform motion. A. Left panel: construction of the potential energy landscape versus the platform angle θ. Solid lines and shadings illustrate group means and SDs in sessions S1 (blue), S2 (orange), and S3 (green). The grey box indicates the boundaries of *NSE* attractor. Right panel: group means (bars) and SDs (whiskers) of the mean potential energy of the *NSE* attractor. B. Left panel: probability density functions (PDFs) of the standardized angular velocity ω' near the *NSE* attractor. Solid lines and shadings illustrate group means and SDs in sessions S1 (blue), S2 (orange), and S3 (green). The grey box indicates the boundaries of *NSE* attractor. Right panel: group means (bars) and SDs (whiskers) of the mean PDFs of angular velocity. (For interpretation of the references to colour in this figure legend, the reader is referred to the web version of this article.)

To confirm this hypothesis, we calculates the number of *successful* trajectories leaving *RSE* or *LSE* and reaching *NSE* (*LSE* → *NSE*, *RSE* → *NSE*, red arrows in Fig. 3A) and the number of *unsuccessful* trajectories leaving *RSE* or *LSE* and reaching their counterpart stable states by passing *NSE* (*LSE* → *RSE*, *RSE* → *LSE*, blue arrows in Fig. 6C). For more details on epoching, please see Methods. Again, one can observe a large deviation of individual trajectories from the group mean in session S1, which becomes less pronounced in S2 and S3, and visually more pronounced in unsuccessful trajectories leaving *RSE*.

To quantify this observation, we compare the time-domain angular velocity profiles using RM ANOVA with within-subject session factors (S1 and S3 conditions) and side effect (starting at *RSE* and at *LSE*). The group mean velocity profiles are presented in the left panel in Fig. 7A. Since we are interested in reducing asymmetry between legs, i.e., how session affects the velocity profiles of different sides, we specifically focus on the interaction of how the side affects changes between sessions. For convenience of comparison, we consider absolute values of the angular velocity. RM ANOVA demonstrates a significant differential effect of the session on the velocity profiles of different sides in the time interval 80–196 ms, where $F_{1,\,15} > F_{\alpha=0.05} = 4.54$. Post-hoc analysis

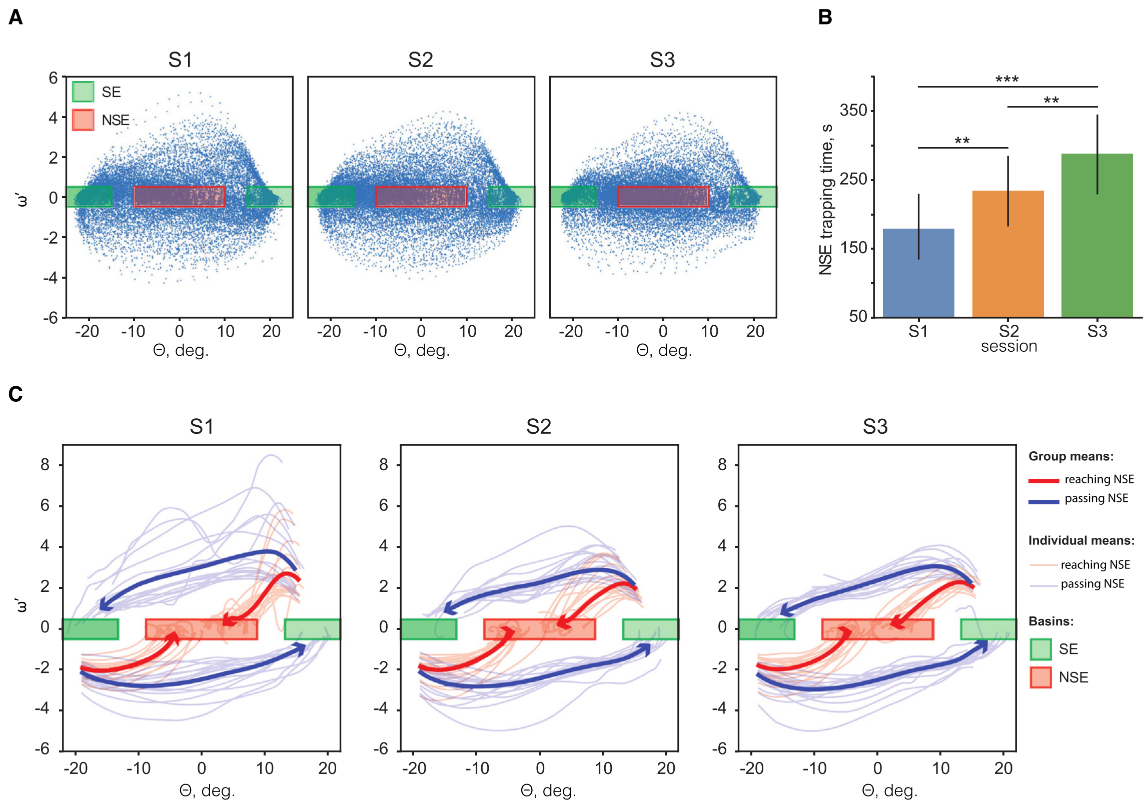

Fig. 6. Phase space analysis of the platform motion. A. A. Individual platform motion trajectory in phase space (θ, ω') in sessions S1, S2, and S3 performed by subject 1. The green and red boxes highlight the boundaries of *SE* and *NSE* attractors. B. Group means (bars) and SDs (whiskers) of the *NSE* attractor trapping time. C. Individual movement trajectories averaged over epochs (semitransparent) and their group means (bold arrows) in sessions S1, S2, and S3. Red trajectories represent the trajectories reaching *NSE*, i.e. *LSE* → *NSE* and *RSE* → *NSE*, while blue ones represent those passing *NSE*, i.e. *LSE* → *RSE* and *RSE* → *LSE*. (For interpretation of the references to colour in this figure legend, the reader is referred to the web version of this article.)

shows that the velocity values averaged over 80–196 ms in session S1 is higher by 0.98 in *RSE* than in *LSE* ($t = 2.694$, $p = 0.017$, $d = 0.67$). On the other hand, no significant difference is found in S2 ($t = 0.33$, $p = 0.75$, $d = 0.08$) and S3 ($t = 0.75$, $p = 0.47$, $d = 0.19$) between the velocity values in the conditions of *RSE* and *LSE*. Group means and SDs of the averaged movement velocity are presented in the right panel in Fig. 7A.

We interpret these results by taking into account that the velocity profiles are highly asymmetric in session S1. In the course of short-term training, this asymmetry is suppressed due to reducing velocity of trajectories leaving the *RSE* position. This behavior can occur due to the fact that the movement trajectories of the *RSE* and *LSE* positions are controlled by the dominant leg (say, right) and non-dominant leg (left) providing the initial push and further transfer of the mass center that regulates the applied momentum. Indeed, confirming this suggestion, we find that the contraction of the left semitendinosus (LST) muscle, quantified by the root mean square of the EMG signal (see Methods), significantly negatively correlates with angular velocity ($r = -0.506$, $p = 0.003$, $power = 0.87$ via RM CORR). In addition, the contraction of the left rectus femoris (LRF) straight head trends to be negatively correlated with angular acceleration measured over a time interval of 0–80 ms ($r = -0.32$, $p = 0.07$, $power = 0.451$ via RM CORR). At the same time, electrophysiological quantitative measurements of other muscles show no significant effect.

Thus, our analysis evidences that short-term body balance training reduces the asymmetry of the balance platform movement.

4. Discussion

In this work, we developed a special balance platform and conducted experiments to study the effect of short-term balance training. Since untrained subjects participated in the experiment, maintaining balance was a rather difficult task which they performed for the first time. The mechanical settings of the balance platform were chosen so that the subjects maintained balance during the first session for a short time (on average, the percentage of balance holding time in relation to the total duration of the first 10-min session was 25.2%) and made a large number of attempts to establish balance. The short workout consisted of three 10-min sessions with 5-min rest breaks in between. To study the behavioral characteristics and dynamics of the platform movement, we used the angle, angular velocity, and angular acceleration of the balance platform.

The training effect consists in increasing the duration of maintained equilibrium. In particular, the average duration increases from 151 s to 265 s from the first to the third session, while 14 out of 16 subjects demonstrate the improving balance. The effect of increasing balance duration is accompanied by a decrease in the platform movement velocity at the beginning of the attempt to reach balance (in the 80–196 ms time interval) from the first to subsequent sessions. This effect is only observed when trying to achieve platform balance with the left leg, while the dynamics of attempts starting with the right leg does not change from session to session. Thus, at the beginning of the experiment, we observe the asymmetry in the platform movement trajectory when the subject starts the movement with his/her left and right legs. This asymmetry was reduced as a result of short-term training of the subjects. We also measure the leg muscular activity using the EMG recording and then calculating RMS for four muscles on each leg. Finally, we find that training is accompanied by an increase in RMS of the left thigh muscles (rectus femoris and semitendinosus muscles) from the first to the third session. At the same time, RM correlation shows a negative relationship between the activity (RMS) of the left thigh muscles and the platform movement characteristics (angular velocity and acceleration).

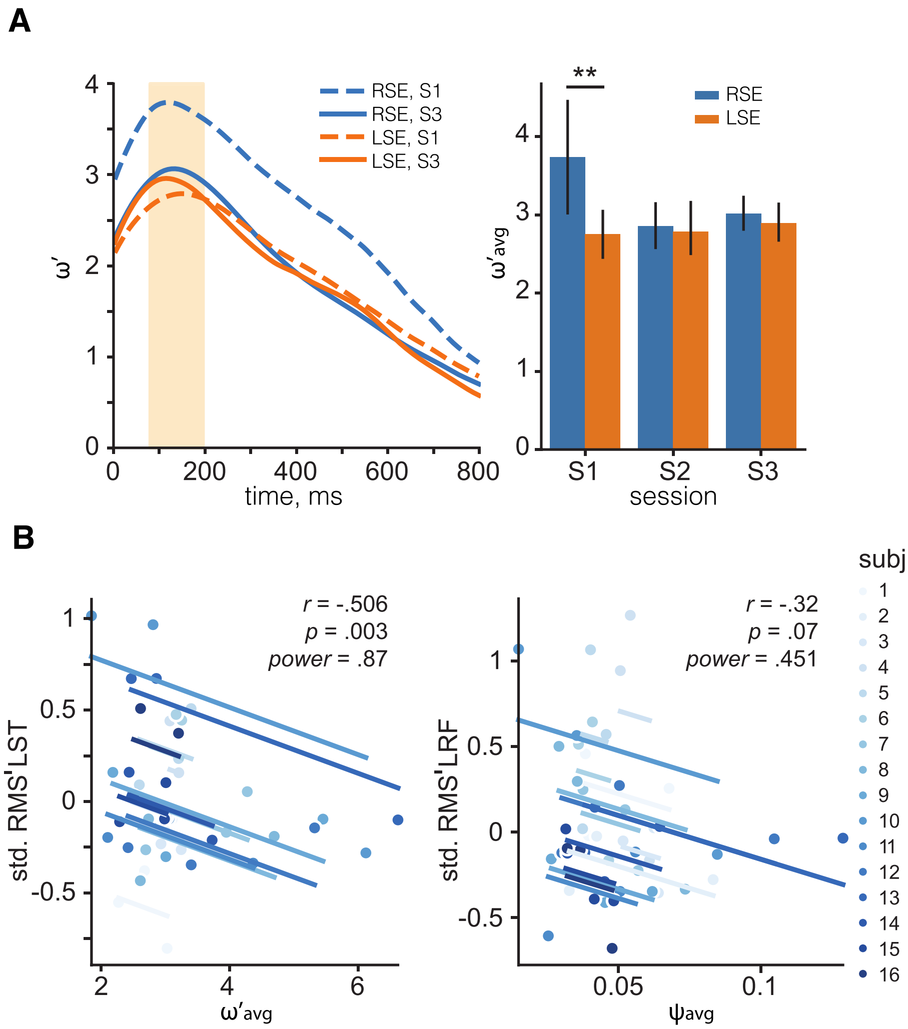

Fig. 7. Asymmetry of the movement trajectory. A. Left panel: group means of the exit velocity profiles for different (Side, Session)-pairs. Shading indicates the time interval of a significant Session*Side effect. Right panel: group means (bars) and SDs (whiskers) of the angular velocity ω_{exit} averaged over the highlighted interval. B. Repeated measures correlation plots. Left panel: Correlation between *RMS′* of the LST muscle and averaged velocity. Right panel: Correlation between *RMS′* of the LRF muscle and averaged angular acceleration ψ_{exit}. Corresponding values of correlation coefficient *r*, significance level *p*, and statistical power are given in the legend.

Thus, our hypothesis about an increase in the efficiency of controlling balance-platform movement as a result of training is confirmed by an increase in the duration of the subject stay near the unstable equilibrium of the balance platform, which is accompanied by a significant change in the left thigh muscle activity. Group averages and standard deviations of the time spent in the vicinity of NSE are shown in Fig. 5B. To explain the increase in the total duration of maintaining equilibrium, we built a model of a double-well potential system reflecting two stable equilibria. The inclusion of experimental trajectories in the model allowed us to calculate the system potential energy for each subject in each session. Based on the potential energy profile analysis, we estimated the mean potential energy for each session, which had a well near the unstable equilibrium at $\theta = 0$ due to human control (see Fig. 1A). Our results demonstrate that the well becomes deeper after the training. Since the platform dynamics itself does not exhibit any potential well near the unstable equilibrium NSE, the increase in the potential well means the improving efficiency of the human control of the balance platform position during the training session. Furthermore, the damping of angular velocity when passing a section equidistant from the boundary positions is a successful strategy to achieve and maintain balance.

We found that the success in maintaining balance during exercise depends on a gradual increase in semitendinosus muscle activity of the left leg, which significantly negatively correlates with the angular exit velocity. One should also pay attention on the negative correlation between the performance acceleration and increased muscle activity of the left rectus femoris muscle. Since the rectus femoris and semitendinosus are both extensors and flexors of the same joint, they simultaneously increase their activity in an attempt to improve movement control through their joint contribution to suppressing the initial movement to get out of a stable equilibrium. The exit rate from the stable equilibrium affects the success of the attempts to maintain balance, while the exit rate is controlled by the rapid effort at the beginning of the attempt (the velocities are shown in Fig. 7B, section 80–196 ms).

It should be noted that the exit trajectory for attempts initiated with the right leg does not change much from session to session, while the trajectory for attempts starting with the left leg improves with training. We believe that this difference is due to the presence of functional asymmetry, since in most cases the right leg was more effectively used as a control leg, since all participants in the experiment had the right leg jerk. Short-term training in our experiment helped to increase the control efficiency of the left leg, which is less involved in daily activities, to the same level as the right leg. During the experiment, the left leg was trained, which provided an optimized trajectory and improved chances for achieving balance.

Similar results for balance exercises were obtained by Rougier et al. [45]. This effect can be explained using the hypothesis that the non-dominant limb has a greater adaptive potential [46]. Other experimental studies involving both the leading and non-leading limb indicate that the non-leading limb shows greater average speed than the leading limb, but the average strength and power of the non-leading limb increase during training [47], although success parameters for precise movement, such as initial direction and accuracy, are initially lower for the non-leading limb [48]. Rehabilitation suggests that many people have neuromotor capacity for improved symmetry of locomotor activity [49]. On the other hand, a decrease in functional asymmetry is a completely natural process for the brain and other structures that adapt their activities during the experiment to changing conditions during the task [50]. Based on the foregoing, it can be concluded that with a short training, the functional asymmetry of the leg muscles decreases, which leads to an increase in the average time to maintain balance.

In their work, Sannicandro with co-authors [51] considered the balance training effect on the functional asymmetry in the leg muscles of tennis athletes. The group of athletes went through a six-week training session that included two 30-min sessions per week. The training sessions consisted of several types of exercises, including jumping, bouncing, rotating on one leg, balancing on an inflatable disc, pillow or step platform (Bosu balance platform). To assess functional asymmetry, sports tests were carried out in the form of jumps and sprints. Based on these experiments, the authors concluded that there is a significant decrease in functional asymmetry of the leg muscles of athletes before and after training. Our results confirm this conclusion in terms of reducing functional asymmetry. In addition, we expand our understanding of this process by demonstrating that the reduction in asymmetry begins after the first training session, and this reduction occurs through improved control of non-dominant limb muscles.

5. Conclusion

In this paper, we have shown that short-term balance training improves the efficiency of adaptive control of multistability of a balance platform by human muscle activity. The phase space analysis of the balance platform movement made it possible to detect an increase in the capture time as the unstable equilibrium stabilizes. We have shown that stability can be achieved even under disequilibrium conditions with a narrow support area (balance bar), despite the fact that individual reactions are unstable. The particle motion model with two potential wells was developed to describe the multistability control of the balance platform during the experiment.

The analysis of the asymmetry of phase trajectories helped us to understand the loss of functional asymmetry in the human body position, which can occur due to the development of non-dominant leg functionality, confirmed by EMG analysis, which showed that more correlated muscle interaction in the non-dominant leg is required to maintain balance more efficiently.

Finally, the results of our research can be used to understand how short-term body balance training suppresses balance platform asymmetry. This leads to more successful outcomes for athletes, such as tennis players who need to control their balance and leg strength. Our results contribute to the advancement in the disclosure of the principles of adaptive control of motor activity aimed at managing the balance, and will be useful for solving a number of applied problems related to improving the quality of human life.

Data availability

All relevant data are within the manuscript is available at [33] link location.

Declaration of competing interest

The authors declare that they have no known competing financial interests or personal relationships that could have appeared to influence the work reported in this paper.

Acknowledgements

This study was supported by the Program of Scientific School Support (grant NSH-589.2022.1.2).

Appendix A. Supplementary data

Supplementary data to this article can be found online at https://doi.org/10.1016/j.chaos.2022.112099.

References

[1] Pisarchik AN, Hramov AE. Multistability in physical and living systems: characterization and applications. Springer; 2022.
[2] Lai Q, Wan Z, Kuate PDK. Modelling and circuit realisation of a new no-equilibrium chaotic system with hidden attractor and coexisting attractors. Electron Lett. 2020; 56:1044–6. https://doi.org/10.1049/el.2020.1630. URL: 10.1049/el.2020.1630.
[3] Ratas I, Pyragas K, Tass PA. Multistability in a star network of kuramoto-type oscillators with synaptic plasticity. Sci Rep. 2021;11. https://doi.org/10.1038/s41598-021-89198-0. URL: 10.1038/s41598-021-89198-0.
[4] Grenzebach J, Wegner TGG, Einh¨auser W, Bendixen A. Pupillometry in auditory multistability. PLOS ONE. 2021;16:e0252370. https://doi.org/10.1371/journal.pone.0252370. URL: doi:10.1371/journal.pone.0252370.
[5] Zhu R, del Rio-Salgado JM, Garcia-Ojalvo J, Elowitz MB. Synthetic multistability in mammalian cells. Science. 2022:375. https://doi.org/10.1126/science.abg9765. URL: 10.1126/science.abg9765.
[6] Daza A, Wagemakers A, Georgeot B, Gu´ery-Odelin D, Sanju´an MAF. Basin entropy: a new tool to analyze uncertainty in dynamical systems. Sci Rep. 2016;6. https://doi.org/10.1038/srep31416. URL: doi:10.1038/srep31416.
[7] Aravind M, Parmananda P, Sinha S. Emergent noise-aided logic through synchronization. Phys Rev E. 2021;104. https://doi.org/10.1103/physreve.104.064207. URL: doi:10.1103/physreve.104.064207.
[8] Pisarchik A, Jaimes-Reátegui R, Rodríguez-Flores C, García-López J, Huerta-Cuellar G, Martín-Pasquín F. Secure chaotic communication based on extreme multistability. J Frankl Inst. 2021;358:2561–75. https://doi.org/10.1016/j.jfranklin.2021.01.013. URL: doi:10.1016/j.jfranklin.2021.01.013.
[9] Pisarchik AN, Feudel U. Control of multistability. Phys Rep. 2014;540:167–218. https://doi.org/10.1016/j.physrep.2014.02.007. URL: doi:10.1016/j.physrep.2014.02.007.
[10] Zhang Z, Chávez JP, Sieber J, Liu Y. Controlling coexisting attractors of a class of non-autonomous dynamical systems. Physica D. 2022;431:133134. https://doi.org/10.1016/j.physd.2021.133134. URL: doi:10.1016/j.physd.2021.133134.
[11] Hayashibe M, Guiraud D, Pons JL, Farina D. Editorial: biosignal processing and computational methods to enhance sensory motor neuroprosthetics. Front Neurosci. 2015;9. https://doi.org/10.3389/fnins.2015.00434. URL:.
[12] Edmunds K, Petersen H, Hassan M, Yassine S, Olivieri A, Barollo F, Fririksdóttir R, Edmunds P, Gíslason M, Fratini A, Gargiulo P. Cortical recruitment and functional dynamics in postural control adaptation and habituation during vibratory proprioceptive stimulation. J Neural Eng. 2019;16:026037.
[13] Solis-Escalante T, van der Cruijsen J, de Kam D, van Kordelaar J, Weerdesteyn V, Schouten A. Cortical dynamics during preparation and execution of reactive balance responses with distinct postural demands. Neuroimage. 2019;188:557–71.
[14] Herold F, Törpel A, Schega L, Müller N. Functional and/or structural brain changes in response to resistance exercises and resistance training lead to cognitive improvements — a systematic review. Eur Rev Aging Phys Act. 2019.;16.
[15] Mierau A, Pester B, H¨ulsdunker T, Schiecke K, Strüder H, Witte H. Cortical correlates of human balance control. Brain Topogr. 2017;30:434–46.
[16] Luu B, Inglis J, Huryn T, der Loos HV, Croft E, Blouin J. Human standing is modified by an unconscious integration of congruent sensory and motor signals. J Physiol. 2012; 590:5783–94.
[17] Annino G, Palazzo F, Lebone P, Caronti A, Lombardo M, Campoli F, Padua E, Iellamo F. The efficacy of plantar stimulation on human balance control. Somatosens Mot Res. 2015;32:200–5.
[18] Strzalkowski NDJ, Ali RA, Bent LR. The firing characteristics of foot sole cutaneous mechanoreceptor afferents in response to vibration stimuli. J Neurophysiol. 2017; 118:1931–42. https://doi.org/10.1152/jn.00647.2016. URL:.
[19] Behm DG, Sanchez JCC. Instability resistance training across the exercise continuum. Sports Health. 2013;5:500–3. https://doi.org/10.1177/1941738113477815.
[20] Marshall P, Murphy B. Changes in muscle activity and perceived exertion during exercises performed on a swiss ball. Sports Appl Physiol Nutr Metab. 2006;31:376–83. https://doi.org/10.1139/h06-006.
[21] Guan Y, Bredin S, Jiang Q, Taunton J, Li Y, Wu N, Wu L, Warburton D. The effect of fatigue on asymmetry between lower limbs in functional performances in elite child taekwondo athletes. J Orthop Surg Res. 2021;16. https://doi.org/10.1186/s13018-020-02175-7. URL:.

[22] Sullivan SW, Fleet NA, Brooks VA, Bido J, Nwachukwu BU, Brubaker PH. Comparison of different functional tests for leg power and normative bilateral asymmetry index in healthy collegiate athletes. Open Access J Sports Med. 2021;12:119–28. https://doi.org/10.2147/oajsm.s315162.
[23] Smith CA, Chimera NJ, Warren M. Association of y balance test reach asymmetry and injury in division i athletes. Med Sci Sports Exerc. 2015;47:136–41. https://doi.org/10.1249/mss.0000000000000380.
[24] Ford KR, Myer GD, Hewett TE. Valgus knee motion during landing in high school female and male basketball players. Med Sci Sports Exerc. 2003;35:1745–50. https://doi.org/10.1249/01.mss.0000089346.85744.d9.
[25] Jacques T, Bini R, Arndt A. Running after cycling induces inter-limb differences in muscle activation but not in kinetics or kinematics. J Sports Sci. 2020;39:154–60. https://doi.org/10.1080/02640414.2020.1809176. URL:.
[26] Plisky PJ, Rauh MJ, Kaminski TW, Underwood FB. Star excursion balance test as a predictor of lower extremity injury in high school basketball players. J Orthop Sports Phys Ther. 2006;36:911–9. https://doi.org/10.2519/jospt.2006.2244. URL:.
[27] Wolpert DM, Diedrichsen J, Flanagan JR. Principles of sensorimotor learning. Nat Rev Neurosci. 2011;12:739–51. https://doi.org/10.1038/nrn3112. URL:.
[28] Elias LJ, Bryden M, Bulman-Fleming M. Footedness is a better predictor than is handedness of emotional lateralization. Neuropsychologia. 1998;36:37–43. https://doi.org/10.1016/s0028-3932(97)00107-3. URL: 10.1016/s0028-3932(97)00107-3.
[29] van Melick N, Meddeler BM, Hoogeboom TJ, van der Sanden MWGN, van Cingel REH. How to determine leg dominance: the agreement between self-reported and observed performance in healthy adults. PLoS One. 2017;12:e0189876. https://doi.org/10.1371/journal.pone.0189876. URL: doi:10.1371/journal.pone.0189876.
[30] https://www.st.com/resource/en/datasheet/lis331dlh.pdf.
[31] Rosati S, Ghislieri M, Dotti G, Fortunato D, Agostini V, Knaflitz M, Balestra G. Evaluation of muscle function by means of a muscle-specific and a global index. MDPI AG. 2021;21:7186.
[32] Kendall FP, McCreary EK, Provance PG, Rodgers MM, Romani WA. Muscles: testing and function with posture and pain. Williams and Wilkins Lippincott; 2005. URL: doi:10.1016/j.physd.2021.133134.
[33] Khorev V, Grubov VV, Kurkin SA, Maksimenko V, Hramov AE. Emg dataset for the analysis of equilibrium-related muscle activity during a series of balance platform tasks performance. Figshare. 2020. https://doi.org/10.6084/m9.figshare.13108067.
[34] Pontryagin LS. Mathematical theory of optimal processes. London, England: Routledge; 2018.
[35] Verd B, Crombach A, Jaeger J. Classification of transient behaviours in a time-dependent toggle switch model. BMC Syst Biol. 2014;8. https://doi.org/10.1186/1752-0509-8-43. doi:10.1186/1752-0509-8-43.
[36] Livina VN, Kwasniok F, Lenton TM. Potential analysis reveals changing number of climate states during the last 60 kyr. Clim Past. 2010;6:77–82.
[37] Hirota M, Holmgren M, Van Nes EH, Scheffer M. Global resilience of tropical forest and savanna to critical transitions. Science. 2011;334:232–5.
[38] Lahti L, Salojärvi J, Salonen A, Scheffer M, De Vos WM. Tipping elements in the human intestinal ecosystem. Nat Commun. 2014;5:1–10.
[39] Curtin P, Austin C, Curtin A, Gennings C, Figueroa-Romero C, Mikhail KA, Botero TM, Goutman SA, Feldman EL, Arora M. Dysregulated biodynamics in metabolic attractor systems precede the emergence of amyotrophic lateral sclerosis. PLoS Comput Biol. 2020;16:e1007773.
[40] Xie Q, Jiang Z, Luo Q. Relationship of root mean square value of electromyography and isometric torque of quadriceps in normal subjects. Rehabil Med. 2016;26:25. https://doi.org/10.3724/sp.j.1329.2016.03025. URL:.
[41] Giannasi LC, Politti F, Dutra MTS, Tenguan VLS, Silva GRC, Mancilha GP, da Silva DB, Oliveira LVF, Oliveira CS, Amorim JBO, Salgado MAC, Gomes MF. Intra-day and inter-day reliability of measurements of the electromyographic signal on masseter and temporal muscles in patients with down syndrome. J Sports Sci Med. 2020.;10.
[42] Bakdash JZ, Marusich LR. Repeated measures correlation. Front Psychol. 2017;8:456.
[43] Jasp. https://jasp-stats.org/.
[44] Sadeghi H, Allard P, Prince F, Labelle H. Symmetry and limb dominance in able-bodied gait: a review. Gait Posture. 2000;12:34–45.
[45] Rougier P, Perennou D. A postural control in healthy young adults using a double seesaw device. J Biomech. 2019;83:214–20.
[46] Yokoi A, Hirashima M, Nozaki D. Lateralized sensitivity of motor memories to the kinematics of the opposite arm reveals functional specialization during bimanual actions. J Neurosci. 2014;34:9141–51. https://doi.org/10.1523/jneurosci.2694-13.2014. URL:.
[47] Zuoza A, Skurvydas A, Mickeviciene D, Gutnik B, Zouzene D, Penchev B, Pencheva S. Behavior of dominant and non dominant arms during ballistic protractive target-directed movements. Hum Physiol. 2009;35:576–84. https://doi.org/10.1134/s0362119709050090. URL:.
[48] Pan Z, van Gemmert AW. The direction of bilateral transfer depends on the performance parameter. Hum Mov Sci. 2013;32:1070–81. URL: 10.1016%2Fj.humov.2012.02.013.
[49] Lewek MD, Braun CH, Wutzke C, Giuliani C. The role of movement errors in modifying spatiotemporal gait asymmetry post stroke: a randomized controlled trial. Clin Rehabil. 2017;32:161–72. https://doi.org/10.1177/0269215517723056. URL:.
[50] Sebastjan A, Skrzek A, Ignasiak Z, Sławińska T. Age-related changes in hand dominance and functional asymmetry in older adults. PLOS ONE. 2017;12:e0177845. https://doi.org/10.1371/journal.pone.0177845. URL:.
[51] Sannicandro I, Cofano G, Rosa R, Piccinno A. Balance training exercises decrease lower-limb strength asymmetry in young tennis players. Sci Rep. 2014;1:397–402.